Optics Communications 328 (2014) 96–101

Contents lists available at ScienceDirect

Optics Communications

journal homepage: www.elsevier.com/locate/optcom

Carrier-envelope phase control electron transport in an asymmetric double quantum dot irradiated by a few-cycle pulse

Wen-Xing Yang [a,b,*], Ai-Xi Chen [c], Hao Guo [a], Yanfeng Bai [a], Ray-Kuang Lee [b]

[a] Department of Physics, Southeast University, Nanjing 210096, China
[b] Institute of Photonics Technologies, National Tsing-Hua University, Hsinchu 300, Taiwan
[c] Department of Applied Physics, School of Basic Science, East China Jiaotong University, Nanchang 330013, China

ARTICLE INFO

Article history:
Received 26 February 2014
Received in revised form
23 April 2014
Accepted 27 April 2014
Available online 9 May 2014

Keywords:
Quantum dot
Electron transport
Carrier-envelope phase
Few-cycle pulse
Quantum interference

ABSTRACT

We propose a theoretical scheme to coherently control the transport of a single electron in an asymmetric double-quantum-dot system. The single-electron transport originates from the intrinsic interplay between the externally applied few-cycle pulse and the inter-dot tunneling. Solving the equations of motion for dot-density matrix, we reveal numerically that the current exhibits a significant dependence on the carrier-envelope phase (CEP) of the few-cycle pulse, which is similar to the magnetic flux controlled coherent transport in an Aharnov–Bohm (AB) interferometer. As a result, by varying the CEP of the pulse one can suppress or enhance the current either instantaneously or periodically. Our results illustrate the potential to utilize few-cycle pulses for excitation in quantum dot systems through the CEP control, as well as a guidance in the design for possible experimental implementations.

1. Introduction

In recent years, it has been realized that the phase of electromagnetic (EM) fields can provide a powerful technique to control or manipulate matters. The method of phase control is associated with the coherent interaction between EM fields and matters, which has already been applied to a variety of different systems [1–7]. Phase dependent phenomena are demonstrated by controllable population dynamics [3], suppressed spontaneous emission [4], and coherent transport in coupled tunneling systems [5,6].

Instead of atomic and molecular systems, solid-state media, especially the quantum dot (QD) structures, have attracted significant research attention due to their potential applications in the development of novel optoelectronic devices and solid-state quantum information science [8]. In QD systems, to manipulate electrons an external magnetic flux is applied firstly to implement possible coherent phase controls. However, it is technologically difficult to confine a strong magnetic field within a very small region, which might be a crucial obstacle for its future applications in quantum processing and computation. Therefore, it is a reasonable choice to replace the magnetic field by some source more easy to control. A natural idea is to use the phase of applied EM fields to control the coherent transport between QD systems, which has revealed many interesting phenomena ranging from photon-assisted tunneling to charge/spin pumping [9–17]. In a recent experiment, microwave spectroscopy has been measured in coupled QDs [18], and the photon-assisted resonances, which involve the emission or absorption of a microwave photon, are found when applying a modulated gate voltage. Some other systems based on time-dependent influences also give rise to promising physical phenomena and applications [19–23].

Meanwhile, tremendous progress in the generating of ultra-short pulses in the few-cycle regime allows one to explore a new class of phase-dependent phenomena. The relative phase difference between the carrier wave and the pulse envelope, which is the so-called carrier-envelope phase (CEP), has many distinctive observable features. Both experimental and theoretical studies have revealed that the CEP of few-cycle pulses indeed plays an important role in the light-matter interactions [24–40]. In this work, we propose a scheme for controlling single-electron transport in an asymmetric double QD system. The coherent transport is externally controlled by applying a few-cycle pulse with an adjustable CEP. We demonstrate that the single-electron transport is in fact the result of the intrinsic interplay between the external few-cycle pulse and the inter-dot tunnel coupling. In particular, we further show that the current can be periodically suppressed or enhanced by modulating the CEP. Our study provides an efficient tool to manipulate the quantum dynamics in QD systems with an adjustable CEP.

2. Model and equations of motion

The present QD system is given in Fig. 1. This device is composed of two different QDs (marked as the left (L) and right

* Corresponding author. Tel.: +86 2552090605-8407
E-mail addresses: wenxingyang@seu.edu.cn, wenxingyang2@126.com (W.-X. Yang).

http://dx.doi.org/10.1016/j.optcom.2014.04.066
0030-4018/

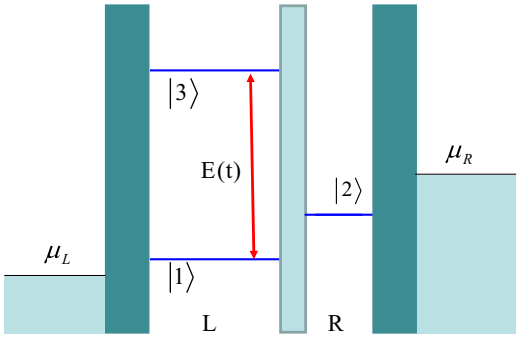

Fig. 1. Schematic diagram of a three-level system which consists of the ground state $|1\rangle$ and the first excited state $|3\rangle$ in the left dot, and the ground state $|2\rangle$ in the right dot in an asymmetric double QD structure. The ground state $|1\rangle$ in the left dot is coupled resonantly to the excited state $|3\rangle$ by a few-cycle pulse $E(t)$.

(R) dots) and two normal metal leads. The size of the right dot is assumed to be much smaller than that of the left one, therefore the energy spacing of it is much larger than that of the left one. The ground state $|1\rangle$ and the first excited state $|3\rangle$ of the left dot and the other ground state $|2\rangle$ of the right dot form a three-level system. Such kind of QD configuration can be realized by a quantum heterostructure consisting of different semiconductor materials (GaAs/AlGaAs). Metal gates could be deposited on the top of a GaAs/AlGaAs heterostructure with a two-dimensional electron gas about 100 nm below the surface [8]. Generically, Coulomb charging energies are of a few meV and they are the largest energy scales. Hence the states associated with more than one additional transport electron can be safely neglected [41–43]. Typical energy difference between the ground state $|1\rangle$ and the first excited state $|3\rangle$ is of the order of several meV [8]. The states $|1\rangle$ and $|3\rangle$ are both coupled to the state $|2\rangle$ via the tunneling through the barrier. The transition between the states $|1\rangle$ and $|3\rangle$ themselves is resonantly driven by a few-cycle pulse characterized by the electric field [25] $E(t)$, which is further defined via the vector potential, $E(t)=-\partial A(t)/\partial t$. This definition guarantees that the vector potential $A(t)$ vanishes at $t=\pm\infty$, or equivalently, the pulse area under $E(t)$ over the entire pulse duration becomes exactly zero [44], which excludes unphysical results. Specifically we assume that the vector potential has a Gaussian temporal envelope, i.e.,

$$A(t)=A_0 e^{-(2\ \ln 2)(t-2\tau)^2/\tau^2}\sin(\omega t+\varphi), \tag{1}$$

where A_0 is the peak of the pulse envelope, ω is the carrier frequency ($2\pi/\omega$ corresponds to an optical oscillation cycle time), and φ is the CEP. The CEP describes the offset of the peak laser pulse relative to the peak position of the envelope. In Eq. (1), we have assumed that the temporal intensity profile is Gaussian temporal envelope with pulse duration τ (full width at half maximum (FWHM)).

In the present system, the effective Hilbert space can be thought of as being spanned by four basis states: $|0\rangle$ (no electron in both dots), $|1\rangle$ (one electron in the ground state of the left dot), $|2\rangle$ (one electron in the ground state of the right dot), and $|3\rangle$ (one electron in the excited state of the left dot). The total Hamiltonian of the system can be expressed in the form [8]

$$H=H_{D0}+H_{DL}+H_{DT}+H_B+H_{ep}. \tag{2}$$

The first term is the free Hamiltonian of the two QDs,

$$H_{D0}=\sum_{j=1,2,3}\epsilon_j|j\rangle\langle j|, \tag{3}$$

where ϵ_j represents the energy of the state $|j\rangle$ $(j=1,2,3)$. The second term describes the interaction between the left dot and a few-cycle pulse,

$$H_{DL}=-\Omega\xi(t)|1\rangle\langle 3|+H.c., \tag{4}$$

where $\xi(t)=\omega^{-1}\partial[e^{-(2\ \ln 2)(t-2\tau)^2/\tau^2}\sin(\omega t+\varphi)]/\partial t$. The Rabi frequency for the transition $|1\rangle\leftrightarrow|3\rangle$ is denoted by $2\Omega=\mu_{13}\omega A_0/\hbar$, with μ_{13} being the corresponding transition dipole moment. The third term describes the coupling Hamiltonian of the dots through the tunneling effect,

$$H_{DT}=\kappa_{12}|1\rangle\langle 2|+\kappa_{32}|3\rangle\langle 2|+H.c., \tag{5}$$

where κ_{ij} is the tunneling coefficient between the states $|i\rangle$ and $|j\rangle$. The fourth term represents the interaction between the leads and the dots and the interaction between the photon modes and the left dot,

$$H_B=\sum_{k,\eta=L,R}\varepsilon_{k,\eta}c^\dagger_{k,\eta}c_{k,\eta}+\sum_{q\nu}\omega_q a^\dagger_{q\nu}a_{q\nu}+\sum_k[V_{kL}c^\dagger_{kL}(|0\rangle\langle 1|+|0\rangle\langle 3|)+V_{kR}c^\dagger_{kR}|0\rangle\langle 2|+H.c.]+\sum_{q\nu}(V_{q\nu}|3\rangle\langle 1|a^\dagger_{q\nu}+H.c.), \tag{6}$$

where $c_{k\eta}$ is the annihilation operator of electrons in the lead η $(\eta=L,R)$, and $a_{q\nu}$ is the annihilation operator of photons with momentum q and polarization ν. $V_{k\eta}$ denotes the coupling strength of the interaction between electrons in the QDs and the leads η. For simplicity, we have assumed that both levels in the left dot interact with the lead L via the same strength. The final term

$$H_{ep}=\sum_Q\frac{1}{2}g_Q\sigma_{z1}(a_{-Q}+a^\dagger_Q)+\sum_Q\omega_Q a^\dagger_Q a_Q+\sum_p\frac{1}{2}g_p\sigma_{z2}(a_{-p}+a^\dagger_p)+\sum_p\omega_p a^\dagger_p a_p \tag{7}$$

describes the coupling of phonons to the charge density which has been found to be the dominant interacting mechanism in a single two-level dot and in the double QDs. Here $\sigma_{z1}=(|3\rangle\langle 3|-|1\rangle\langle 1|)$, $\sigma_{z2}=(|2\rangle\langle 2|-|1\rangle\langle 1|)$, $a^\dagger_Q(a^\dagger_p)$ is the creation operator of phonons with frequency $\omega_Q(\omega_p)$, and $g_Q(g_p)$ is the coupling strength of the interaction between electrons and phonons [45].

The transition rates between the states of the left lead and the two states of the left dot are expressed as $\Gamma^\pm_{Lj}=\Gamma_L f^\pm_j(\epsilon_j)$ $(j=1,3)$, where $\Gamma_L=2\pi\sum_k|V_{kL}|^2\delta(\epsilon_j-\varepsilon_{kL})$ and $f^\pm_j(\epsilon)=\{1+\exp[\pm(\epsilon-\mu_L)/k_BT\}^{-1}$ is the Fermi distribution function of the left reservoir. Here μ_L is the chemical potential, and $\pm$ corresponds to the occupied/empty state of the left lead. More specifically, Γ^+_{Lj} represents the tunneling rate of the transition of electrons from the left lead into the state $|j\rangle$, while Γ^-_{Lj} represents the tunneling rate of the inverse process. Furthermore, here we only consider a low bias configuration where μ_L is well below the two energy levels of the left dot [11,17], hence the Fermi distribution functions can be approximated as $f^+_L(\epsilon_j)=0$ and $f^-_L(\epsilon_j)=1$. In this case, the transition rates are further simplified as $\Gamma^-_{Lj}=\Gamma_L$ and $\Gamma^+_{Lj}=0$.

Now we consider the transition of electrons in the "right" part of the system. We assume that the chemical potential μ_R of the right lead is well above the energy level of the right dot. By similar deduction, the tunneling rate of transition of electrons from the state $|2\rangle$ to the right lead is given by $\Gamma^-_R=0$, and the tunneling rate of the inverse process is approximated as $\Gamma^+_R=\Gamma_R$ [11,17]. For simplicity, we assume that the dot-lead tunneling rates satisfy $\Gamma_L=\Gamma_R=\Gamma$. Under the assumption of weak coupling between the QDs and the leads, the behavior of the double QDs in the sequential regime can be described in terms of the density operator of the system. After adiabatically eliminating the reservoir operators c_{kR}, c_{kL}, $a_{q\nu}$, a_p, a_Q and employing the Born–Markov approximation, the master equations for the density matrix of the system can be written as [49]

$$\frac{\partial\rho_{33}}{\partial t}=-\gamma_3\rho_{33}-\Gamma\rho_{00}+i\Omega\xi(t)(\rho_{13}-\rho_{31})+i\kappa_{32}(\rho_{23}-\rho_{32}), \tag{8}$$

$$\frac{\partial\rho_{11}}{\partial t}=\gamma_3\rho_{33}-\Gamma\rho_{00}-i\Omega\xi(t)(\rho_{31}-\rho_{13})+i\kappa_{12}(\rho_{21}-\rho_{12}), \tag{9}$$

$$\frac{\partial\rho_{22}}{\partial t}=-\gamma_2\rho_{22}+\Gamma\rho_{22}-i\kappa_{12}(\rho_{21}-\rho_{12})-i\kappa_{32}(\rho_{23}-\rho_{32}), \tag{10}$$

$$\frac{\partial\rho_{13}}{\partial t}=-\frac{\gamma_3+\beta}{2}\rho_{13}+i\Omega\xi(t)(\rho_{33}-\rho_{11})+i\kappa_{32}\rho_{21}-i\kappa_{12}\rho_{23}, \tag{11}$$

$$\frac{\partial\rho_{12}}{\partial t}=-\left[\frac{\gamma_2+\beta-\Gamma}{2}+i\left(\Delta+\frac{\omega}{2}\right)\right]\rho_{12}+i\kappa_{12}(\rho_{11}-\rho_{22}) +i\kappa_{32}\rho_{13}-i\Omega\xi(t)\rho_{32}, \tag{12}$$

$$\frac{\partial\rho_{23}}{\partial t}=-\left[\frac{\gamma_2+\gamma_3+\beta-\Gamma}{2}-i\left(\Delta+\frac{\omega}{2}\right)\right]\rho_{23}-i\kappa_{12}\rho_{13} +i\kappa_{32}(\rho_{22}-\rho_{33})-i\Omega\xi(t)\rho_{21}, \tag{13}$$

with $\rho_{00}+\rho_{11}+\rho_{22}+\rho_{33}=1$, where the detuning frequency $\Delta=\varepsilon_2-\varepsilon_1-\omega/2$ is tunable if an external bias is applied perpendicularly to the barrier layer. The diagonal elements of the density matrix, ρ_{jj} $(j=0,1,2,3)$, correspond to the populations of electrons on the states $|j\rangle$. The off-diagonal density matrix elements describe the coherent superposition of the three levels. The damping terms including population decay rates and related dephasing rates are added phenomenologically in the above equations. The population decay rate γ_j for the state $|j\rangle$ comes primarily from the interaction between the QDs and the vacuum EM fields. The dephasing rate β arises from the phonon emission and scattering, and the interaction between electrons and phonons [42]. A more complete theoretical treatment in which the incoherent relaxation processes are taken into account is thought to be interesting [42,45–48], but this goes well beyond the scope of this paper.

We can solve Eqs. (8)–(13) numerically to obtain the time-dependent current flowing from the right lead to the QD in the sequential regime [49,50],

$$I(t)/e=\Gamma\rho_{00}(t). \tag{14}$$

According to the law of current conservation, the time-dependent current flowing from the QD to the left lead can be written as

$$I(t)/e=\Gamma[\rho_{11}(t)+\rho_{33}(t)]. \tag{15}$$

Under our approximation that $\mu_L\ll\epsilon_{1,3}$ and $\mu_R\gg\epsilon_2$, electrons can tunnel out from both the excited and ground states of the left QD. Therefore these two states must contribute to the transport, as shown in Fig. 1. According to Eq. (15), the current contributions of the two states are equivalent. For convenience, we separate the current into $I(t)/e=I_1(t)/e+I_3(t)/e$ where $I_1(t)/e=\Gamma\rho_{11}(t)$ and $I_3(t)/e=\Gamma\rho_{33}(t)$. Therefore, the few-cycle pulse does have a strong effect on the non-equilibrium transport in the present double QD system. We mainly focus on the modulation of the CEP of a few-cycle pulse φ on the current. In the following section, we will directly examine the final current $I(\infty)/e\Gamma$ by numerically integrating Eqs. (8)–(13) without making the RWA in the adiabatic basis by means of a fourth-order Runge–Kutta method. Besides, we restrict our calculations within the resonant case of transition $(\epsilon_3-\epsilon_1=\omega)$ and assume $\kappa_{12}=\kappa_{32}=\kappa$ for simplicity.

3. Numerical results and discussion

Here we discuss some implications from our numerical results. Shown in Fig. 2 is the behavior of the resonant few-cycle pulses with the pulse duration $\tau=5$ ps and the carrier frequency $\omega=\epsilon_3-\epsilon_1=4$ meV with the central wavelength $\lambda=0.31$ mm. Thus the pulse corresponds to the few-cycle THz pulses (the number of optical oscillation cycles $N=\tau/(2\pi/\omega)\simeq 5$) [51,52]. It is evident that the electric field as a function of time depends on the CEP, although the envelope is the same for all pulses. One can also see that a phase shift φ of $\pi/2$ changes the peak value of the central oscillation near the envelope maximum considerably. It will be demonstrated later that related physical processes induced by this few-cycle pulse also have strong dependence on the CEP.

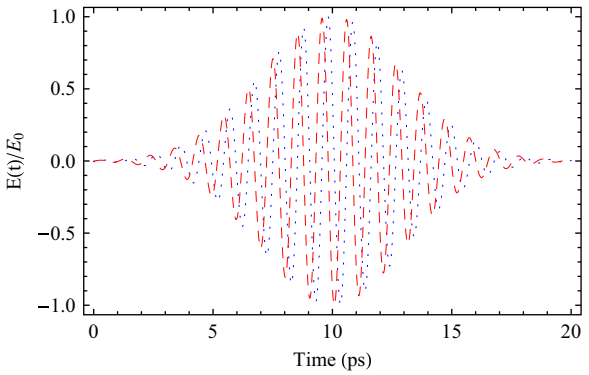

Fig. 2. Time variation of the electric field for few-cycle pulses with a different CEP φ. A comparison between $\varphi=\pi/2$ (dotted-line) and $\varphi=0$ (dashed-line) is shown. Other parameters used are $\tau=5$ ps and $\omega=4$ meV.

To acquire a tentative impression of the properties of $I(\infty)$, we first consider the simple situation that the resonant few-cycle pulse is absent $(\Omega=0)$ and the decay and dephasing effects are not taken into account $(\gamma_2=\gamma_3=\beta=0)$. Fig. 3(a) plots the current $I(\infty)/e\Gamma$ as a function of the detuning Δ under this simplification. It can be seen that the current spectrum exhibits a two-peak structure, as shown by the black solid line. The locations of the two peaks are at $\Delta=\pm\omega/2$, corresponding to the two channels of electron resonant tunneling: $|2\rangle\leftrightarrow|1\rangle$ and $|2\rangle\leftrightarrow|3\rangle$. When $\Delta=-\omega/2$, the electron can only transport from the state $|2\rangle$ to $|1\rangle$ and then a peak appears. This transition is determined by the resonant tunneling κ_{12}. Similarly, if $\Delta=\omega/2$, the main transition channel of the electrons is from the state $|2\rangle$ to $|3\rangle$ and another peak shows up, which is determined by the resonant tunneling κ_{32}. We have restricted our calculation under the condition $\kappa_{12}=\kappa_{32}$, hence the current $I(\infty)/e\Gamma$ (solid-line) consists of two components $I_1(\infty)/e\Gamma$ (dotted-line) and $I_3(\infty)/e\Gamma$ (dashed-line). Both of them contribute equally to the current, thus the current spectrum shows a symmetric two-peak structure, as shown in Fig. 3(a). In a realistic double QD system, the population decay and dephasing rates are generically nonzero. For example we can set $\gamma_2=\gamma_3=\beta=0.001$ meV, and it can be found in Fig. 3(b) that the peak values are lower down. From here on in this paper, we will take into account the effect of the decay and dephasing.

If the transition $|1\rangle\leftrightarrow|3\rangle$ is driven by a few-cycle pulse $(\Omega=0.2$ meV), the current spectrum shows an interesting behavior. Compared to the situation with $\Omega=0$, the two-peak structure becomes asymmetric, while the peak locations remain unchanged, as shown in Fig. 4. When $\varphi=0$ (see Fig. 4(a)), one can find that the right peak is higher than the left one, while one gets the exactly opposite result when $\varphi=\pi/2$ (see Fig. 4(b)). This interesting phenomenon comes from the CEP-dependent quantum interference. When $\Delta=-\omega/2$, there are two transport pathways for the transition channel $|2\rangle\leftrightarrow|1\rangle$. One is simply the single electron tunneling $|2\rangle\leftrightarrow|1\rangle$, which is determined by the tunneling rate κ_{12}. The other is $|2\rangle\leftrightarrow|3\rangle\leftrightarrow|1\rangle$, which is determined by the tunneling rate κ_{32} and the driven field $E(t)$. These two pathways can interfere with each other either constructively or destructively, depending on the CEP φ. The situation with $\Delta=\omega/2$ is quite similar. There are also two transport pathways for the transition channel, either $|2\rangle\leftrightarrow|3\rangle$ or $|2\rangle\leftrightarrow|1\rangle\leftrightarrow|3\rangle$. They are determined by κ_{12} only or by κ_{32} and driven field $E(t)$together, respectively. These two pathways also interfere with each other. Fig. 4 illustrates the interference pattern between two transport pathways for two

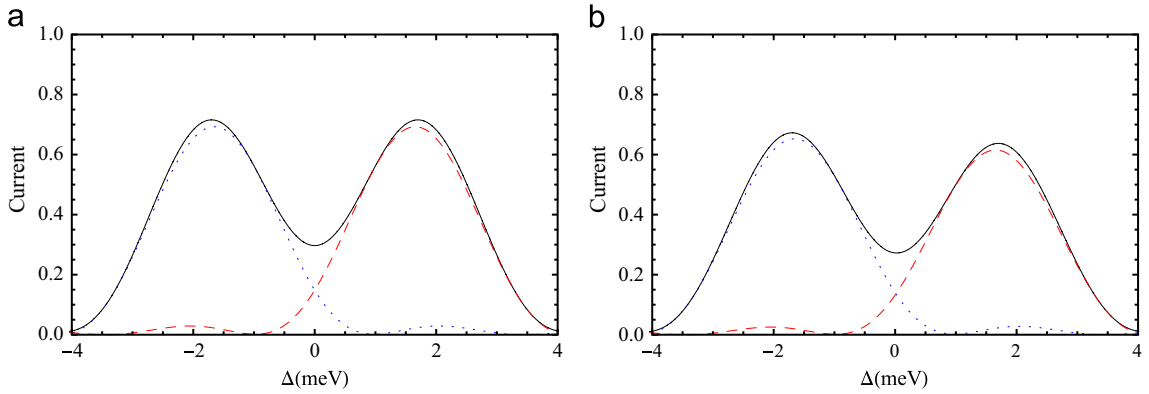

Fig. 3. The final current as a function of detuning frequency Δ in the absence of a few-cycle pulse ($\Omega=0$): the current $I(\infty)/e\Gamma$ (solid-line), $I_1(\infty)/e\Gamma$ (dotted-line), and $I_3(\infty)/e\Gamma$ (dashed-line). A comparison between the cases without and with the decay rates is shown for (a) $\gamma_2=\gamma_3=\beta=0$ and (b) $\gamma_2=\gamma_3=\beta=0.001$ meV, respectively. Other parameters used are $\kappa=0.05$ meV, and $\epsilon_3-\epsilon_1=\omega=4$ meV.

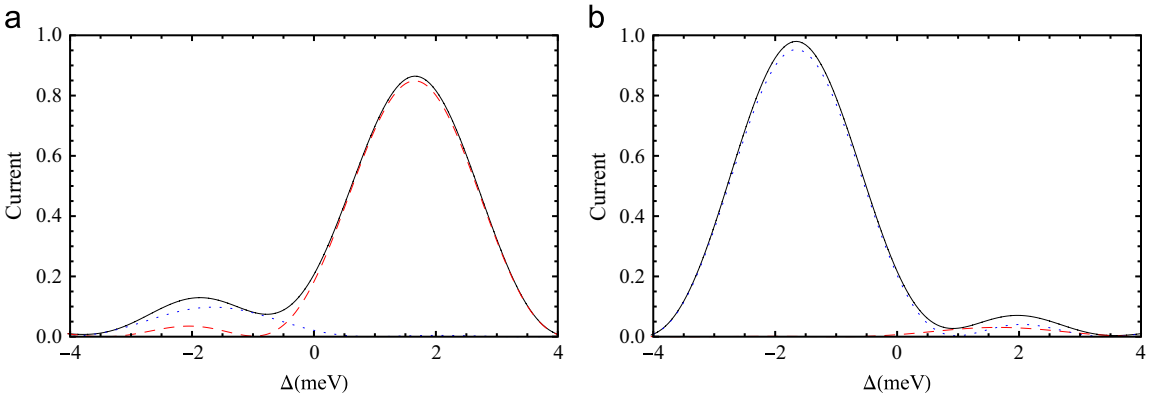

Fig. 4. The final current as a function of detuning frequency Δ in the presence of a few-cycle pulse ($\Omega=0.2$ meV): the current $I(\infty)/e\Gamma$ (solid-line), $I_1(\infty)/e\Gamma$ (dotted-line), and $I_3(\infty)/e\Gamma$ (dashed-line). A comparison between the cases with a different CEP is shown for (a) $\varphi=0$ and (b) $\varphi=\pi/2$. Other parameters used are $\kappa=0.05$ meV, $\gamma_2=\gamma_3=\beta=0.001$ meV, and $\epsilon_3-\epsilon_1=\omega=4$ meV.

transition channels. (a) shows the constructive interference for the transition $|2\rangle\leftrightarrow|3\rangle$ and the destructive interference for the transition $|2\rangle\leftrightarrow|1\rangle$ when $\varphi=0$, while (b) shows the destructive interference for the transition $|2\rangle\leftrightarrow|3\rangle$ and the constructive interference for the transition $|2\rangle\leftrightarrow|1\rangle$ when $\varphi=\pi/2$. It can also be seen that in Fig. 4(a) $I_3(\infty)/e\Gamma$ (dashed-line) gives a larger contribution than $I_1(\infty)/e\Gamma$ (dotted-line), thus the current spectrum exhibits asymmetric peak structure (solid-line). Fig. 4(b) also shows that both the current components $I_1(\infty/e\Gamma)$ (dotted-line) and $I_3(\infty)/e\Gamma$ (dashed-line) unequally contribute to the current peaks.

In order to further explore the dependence of the current on the CEP, we present in Fig. 5 the final current as a function of the CEP of the few-cycle pulse, and the parameters are chosen as $\Omega=0.2$ meV and $\Delta=2$ meV. Obviously, the current spectrum has a strong dependence on the CEP and it can be enhanced and suppressed periodically as the change of the CEP. The current reaches its maxima at $\varphi=k\pi$ $(k=0,1,2)$ and its minima at $\varphi=k\pi/2$. The role of the CEP here is quite similar to the magnetic flux in an AB ring [53]. However, it is quite different from the AB interferometer results from the external bias voltage in an AB ring. Here, the modulation of the current results from quantum interference induced by the few-cycle pulse. But our system shares the same physical background with an AB ring for the phase modulated quantum interference.

For get a better insight into the CEP modulation effect on the global behavior of the current, we present the contour plot of the current in Fig. 6, in which the horizontal and vertical axes correspond to the CEP φ and the electric field amplitude $\hbar\Omega$,

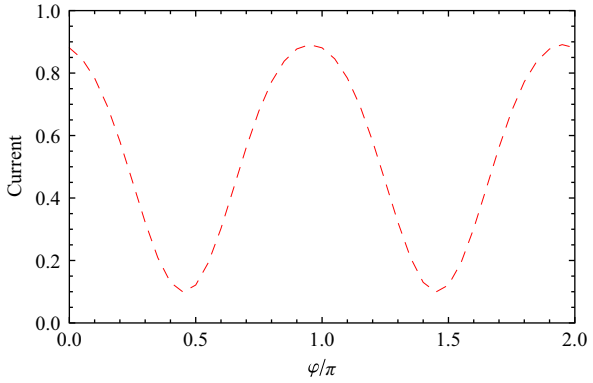

Fig. 5. The final current $I(\infty)/e\Gamma$ as a function of the CEP φ. The parameters used are $\Omega=0.2$ meV, $\Delta=2$ meV, $\gamma_2=\gamma_3=\beta=0.001$ meV, $\epsilon_3-\epsilon_1=\omega=4$ meV, $\tau=5$ ps, and $\kappa=0.05$ meV.

respectively. It can be seen that the maximal (minimum) value of the final current increases (decreases) as Ω increases, which clearly illustrates the feature that the few-cycle pulse with higher intensity leads to more significant modulation of the final current. Plotted in Fig. 7 is the contour map of the current as a function of the CEP φ and the detuning frequency Δ with a fixed electric amplitude $\Omega=0.2$ meV. It can be found that at $\Delta=\pm\omega/2$ the modulation is more pronounced. Besides, the electric field $E(t)$ has the period 2π as a function of CEP, which implies that the current approximately has a period π as a function of CEP, which is clearly shown in Figs. 5–7. In conclusion, it is the quantum interference determined by the CEP that can be used to modulate the current in

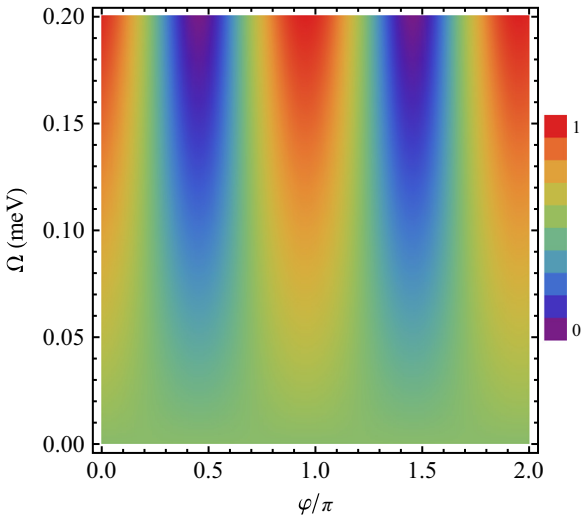

Fig. 6. The contour map of the final current $I(\infty)/e\Gamma$ for the varying CEPs φ and varying electric amplitudes Ω of the few-cycle pulse. The parameters used are $\Delta = 2$ meV, $\gamma_2 = \gamma_3 = \beta = 0.001$ meV, $\epsilon_3 - \epsilon_1 = \omega = 4$ meV, $\tau = 5$ ps, and $\kappa = 0.05$ meV.

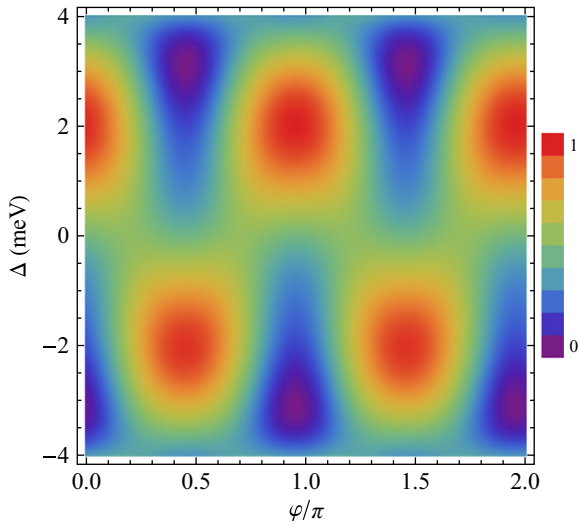

Fig. 7. The contour map of the final current $I(\infty)/e\Gamma$ for the varying CEPs φ and varying detuning frequencies Δ. The parameters used are $\Omega = 0.2$ meV, $\gamma_2 = \gamma_3 = \beta = 0.001$ meV, $\epsilon_3 - \epsilon_1 = \omega = 4$ meV, $\tau = 5$ ps, and $\kappa = 0.05$ meV.

a double QD system. This effect may serve as a CEP controlled current switch.

To visualize the modulation depth of the current modulated by the CEP φ, we introduce the parameter

$$M = \frac{I_{max}(\varphi) - I_{min}(\varphi)}{I_{max}(\varphi) + I_{min}(\varphi)}. \tag{16}$$

From Fig. 5, one can find that the modulation depth M can reach 0.8 if the parameters are fixed as $\Omega = 0.2$ meV, $\Delta = 4$ meV. Furthermore, Figs. 6 and 7 imply that M can be tuned by changing the electric amplitude and detuning frequency. By investigating the effect of few-cycle pulses on the single-electron transport in a double QD system, the pulse width plays an important role at the given carrier frequency ω. It determines the number of cycles of the field in the pulse. In Fig. 8, we plot M as a function of the number of cycles N (in units of optical period of the pulse, i.e., $N = \tau/[2\pi/\omega]$) at a different electric amplitude Ω and detuning frequency Δ. It can be seen that M decreases as the number of cycles increases. This means that the modulation depth strongly depends on the pulse width τ. The longer the pulse width, the smaller the modulation depth, which can be explained by the time-dependent perturbation theory. In addition, Fig. 8(a) shows that M increases as Ω increases, which clearly illustrates the fact that a smaller Rabi frequency induces a smaller modulation which is therefore unfavorable from the viewpoint of the experimental measurement. The lower limit of the Rabi frequency depends on the precision of the measurement of the current [8]. Fig. 8 (b) shows that the detuning frequency Δ has a significant effect on the CEP modulation depth as well. It can be concluded from Fig. 8 that the single-electron transport can be optimized (maximized) by choosing a proper set of detuning Δ, amplitude Ω, and the pulse width τ.

4. Conclusion

In conclusion, we have demonstrated coherent control of the single-electron transport in an asymmetric double QD system driven by a few-cycle pulse by varying the CEP. By numerical simulations, it is clearly shown that the current is extremely sensitive to the CEP if the pulse is in the few-cycle regime. The results suggest that such a system can provide a potential electro-optical method to control the electron transport. A possible experimental implementation for our proposed scheme is to tune the energy levels by applying a gate voltage in an asymmetric QD. Another possible experimental realization is proposed by Fujisawa

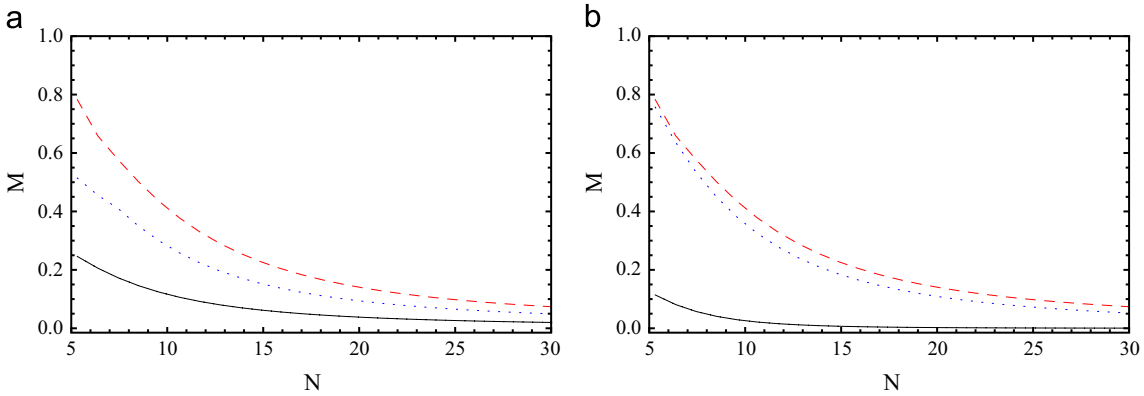

Fig. 8. Modulation depth, M, of the final current, with respect to the CEP, shown as a function of the number of cycles of a few-cycle pulse, $N = \tau/[2\pi/\omega]$, for (a) different electric field amplitudes Ω, i.e., $\Omega = 0.05$ meV (solid-line), $\Omega = 0.1$ meV (dotted-line), and $\Omega = 0.2$ meV (dashed-line), but with a fixed detuning $\Delta = 2$ meV; (b) for different values of detunings Δ, i.e., $\Delta = 0$ (solid-line), $\Delta = -2$ meV (dotted-line), and $\Delta = 2$ meV (dashed-line), but with a fixed field amplitude $\Omega = 0.2$ meV. Other parameters used are $\gamma_2 = \gamma_3 = \beta = 0.001$ meV, $\epsilon_3 - \epsilon_1 = \omega = 4$ meV, and $\kappa = 0.05$ meV.

et al. [42], of which an important requirement is the asymmetric double dot structure. Although the work of Fujisawa et al. is concentrated on a two-level system, it can be easily generalized to the three-level case by applying an adequate external field [54–56] (an additional channel is opened for the transport). Based on the advanced nanofabrication technologies, we believe that our model can be experimentally realized under proper arrangements. It should be noted that our CEP control shares a similar mechanism to that of the magnetic flux controlled interferometer. Moreover, the interaction between the electron and the few-cycle pulse is much easier to manipulate. We believe that the quantum interference or coherence phenomena in other material systems [57–59] besides the QD would also show a similar sensitive CEP dependent effect. Therefore, the CEP controlled quantum interference or coherence shall provide another feasible approach for applications in nanoelectronics and quantum information science.

Acknowledgments

We appreciate useful discussions with Prof. Y. Wu and E. Paspalakis. The research is supported in part by the National Natural Science Foundation of China under Grant nos. 11374050 and 61372102, by Qing Lan project of Jiangsu, and by the Fundamental Research Funds for the Central Universities under Grant nos. 2242012R30011 and 2242013R3008.

References

[1] M. Shapiro, P. Brumer, Rep. Prog. Phys. 66 (2003) 859.
[2] Y. Wu, M.G. Payne, E.W. Hagley, L. Deng, Phys. Rev. A 69 (2004) 063803.
[3] H. Li, V.A. Sautenkov, Y.V. Rostovtsev, M.M. Kash, P.M. Anisimov, G.R. Welch, M.O. Scully, Phys. Rev. Lett. 104 (2010) 103001.
[4] F. Ghafoor, S.Y. Zhu, M.S. Zubairy, Phys. Rev. A 62 (2000) 013811.
[5] G. Platero, R. Aguado, Phys. Rep. 395 (2004) 1.
[6] J.F. Dynes, E. Paspalakis, Phys. Rev. B 73 (2006) 233305.
[7] Y. Wu, X. Yang, Phys. Rev. A 56 (1997) 2443.
[8] J.P. Bird, Electron Transport in Quantum Dots, Springer, Berlin, 2003.
[9] S. Selstø, M. Førre, Phys. Rev. B 74 (2006) 195327.
[10] A. Fountoulakis, A.F. Terzis, E. Paspalakis, J. Appl. Phys. 106 (2009) 074305.
[11] G. Li, S. Wu, J. Zhu, J. Opt. Soc. Am. B 27 (2010) 1634.
[12] P. Trocha, Phys. Rev. B 82 (2010) 115320.
[13] S. Kumar, Q. Hu, Phys. Rev. B 80 (2009) 245316.
[14] S.K. Watson, R.M. Potok, C.M. Marcus, V. Umansky, Phys. Rev. Lett. 91 (2003) 258301.
[15] J. Splettstoesser, M. Governale, J. Konig, R. Fazio, Phys. Rev. Lett. 95 (2005) 246803.
[16] E. Cota, R. Aguado, G. Platero, Phys. Rev. Lett. 94 (2005) 107202.
[17] Y.Y. Liao, D.S. Chuu, Y.N. Chen, Phys. Rev. B 75 (2007) 125325.
[18] T.H. Oosterkamp, T. Fujisawa, W.G. van der Wiel, K. Ishibashi, R.V. Hijman, S. Tarucha, L.P. Kouwenhoven, Nature (London) 395 (1998) 873.
[19] L.A. Openov, Phys. Rev. B 60 (1999) 8798.
[20] U. Hohenester, F. Troiani, E. Molinari, G. Panzarini, C. Macchiavello, Appl. Phys. Lett. 77 (2000) 1864.
[21] T. Brandes, F. Renzoni, Phys. Rev. Lett. 85 (2000) 4148.
[22] S. Komiyama, O. Astafiev, V. Antonov, T. Kutsuwa, H. Hirai, Nature (London) 403 (2000) 405.
[23] A. Zrenner, E. Beham, S. Stufler, F. Findeis, M. Bichler, B. Abstreiter, Nature (London) 418 (2002) 612.
[24] T. Nakajima, S. Watanabe, Phys. Rev. Lett. 96 (2006) 213001.
[25] Y. Wu, X. Yang, Phys. Rev. A 76 (2007) 013832.
[26] Y. Wu, X. Yang, Phys. Rev. Lett. 98 (2007) 013601.
[27] X.-T. Xie, M. Macovei, M. Kiffner, C.H. Keitel, J. Opt. Soc. Am. B 26 (2009) 1912.
[28] P. Huang, X.T. Xie, X.Y. Lu, J.H. Li, X. Yang, Phys. Rev. A 79 (2009) 043806.
[29] N. Doslic, Phys. Rev. A 74 (2006) 013402.
[30] T. Cheng, A. Brown, Phys. Rev. A 70 (2004) 063411.
[31] A. Gandman, L. Chuntonov, L. Rybak, Z. Amitay, Phys. Rev. A 75 (2007) 031401 (R).
[32] N. Cui, Y. Xiang, Y. Niu, S. Gong, New J. Phys. 12 (2010) 013009.
[33] H. Yao, Y. Niu, Y. Peng, S. Gong, Opt. Commun. 284 (2011) 4059.
[34] T.M. Fortier, P.A. Roos, D.J. Jones, S.T. Cundiff, R.D.R. Bhat, J.E. Sipe, Phys. Rev. Lett. 92 (2004) 147403.
[35] C. Zhang, X. Song, W. Yang, Z. Xu, Opt. Express 16 (2008) 11487.
[36] C. Van Vlack, S. Hughes, Phys. Rev. Lett. 98 (2007) 167404.
[37] W.-X. Yang, X. Yang, R.-K. Lee, Opt. Express 17 (2009) 15402.
[38] Y.Y. Lin, I.Hong. Chen, R.-K. Lee, Phys. Rev. A 83 (2011) 043828.
[39] J. Li, R. Yu, P. Huang, A. Zheng, X. Yang, Phys. Lett. A 373 (2009) 1896.
[40] J. Cheng, J. Zhou, Phys. Rev. A 64 (2001) 065402.
[41] T. Brandes, T. Vorrath, Phys. Rev. B 66 (2002) 075341.
[42] T. Fujisawa, T. Hayashi, S. Sasaki, Rep. Prog. Phys. 69 (2006) 759.
[43] W. Chu, S. Duan, J.L. Zhu, Appl. Phys. Lett. 90 (2007) 222102.
[44] S. Chelkowski, A.D. Bandrauk, Phys. Rev. A 65 (2002) 061802(R).
[45] G. Kießlich, E. Scholl, T. Brandes, F. Hohls, R.J. Haug, Phys. Rev. Lett. 99 (2007) 206602.
[46] K. Shen, M.W. Wu, Phys. Rev. B 76 (2007) 235313.
[47] Y.Y. Wang, M.W. Wu, Phys. Rev. B 77 (2008) 125323.
[48] M.W. Wu, J.H. Jiang, M.Q. Weng, Phys. Rep. 493 (2010) 61.
[49] T. Brandes, F. Renzoni, R.H. Blick, Phys. Rev. B 64 (2001) 035319.
[50] B. Dong, H.L. Cui, X.L. Lei, Phys. Rev. B 69 (2004) 035324.
[51] L. Razzari, F.H. Su, G. Sharma, F. Blanchard, A. Ayesheshim, H.-C. Bandulet, R. Morandotti, J.-C. Kieffer, T. Ozaki, M. Reid, F.A. Hegmann, Phys. Rev. B 79 (2009) 193204.
[52] J.L. Tomaino, A.D. Jameson, Yun-Shik Lee, J.P. Prineas, J.T. Steiner, M. Kira, S. W. Koch, Solid-State Electron. 54 (2010) 1125.
[53] Y. Aharonov, D. Bohm, Phys. Rev. 115 (1963) 485.
[54] I.H. Chan, R.M. Westervelt, K.D. Maranowski, A.C. Gossard, Appl. Phys. Lett. 80 (2002) 1818.
[55] K. Ono, D.G. Austing, Y. Tokura, S. Tarucha, Science 297 (2002) 1313.
[56] H. Qin, F. Simmel, R.H. Blick, J.P. Kotthaus, W. Wegscheider, M. Bichler, Phys. Rev. B 63 (2001) 035320.
[57] Z. Zheng, C. Zhao, S. Lu, Y. Chen, Y. Li, H. Zhang, S. Wen, Opt. Express 20 (2012) 23201.
[58] H. Zhang, S.B. Lu, J. Zheng, J. Du, S.C. Wen, D.Y. Tang, K.P. Loh, Opt. Express 22 (2014) 7249.
[59] S. Chen, C. Zhao, Y. Li, H. Huang, S. Lu, H. Zhang, S. Wen, Opt. Mater. Express 4 (2014) 587.